48

AAS 95-001

THE STANFORD RELATIVITY MISSION "NIOBIUM BIRD": VERIFICATION OF THE SCIENCE MISSION BY EXPERIMENTAL APPLICATION OF A NEW NONLINEAR ESTIMATION ALGORITHM

Gordon T. Haupt, Gregory M. Gutt, James M. Lockhart, N. Jeremy Kasdin, George M. Keiser, Bradford W. Parkinson*

The Stanford Relativity Mission is one of NASA's most challenging experiments. It will check previously untested aspects of Einstein's General Theory of Relativity by measuring, over the course of a one year experiment, the directional change of an Earth-orbiting gyroscope's spin axis relative to inertial space as defined by the fixed stars. According to general relativity, the spin axis undergoes two orthogonal precessions of magnitude 6.6 and 0.04 arcseconds per year for a polar 650 km orbit. These tiny angles will be measured to sub-milliarcsecond accuracy, a requirement which puts extreme constraints on the gyroscopes and the readout system used to measure the spin axis direction. Given these requirements, it is crucial that the gyroscope, readout system and data reduction performance be verified to the fullest extent possible on the ground before the mission is flown.

Analogous to the "Iron Birds" of the aircraft industry, the Niobium Bird is intended to provide precisely this end-to-end verification. The Niobium Bird (the name refers to the extensive use of niobium in the experiment) is a hardware-in-the-loop simulation, integrating computer simulation of the science signal with prototypical readout hardware. A data reduction scheme uses the experimental data to obtain estimates of the relativistic drifts, which are then compared with the simulation parameters to determine the accuracy of the system. This paper presents the latest results from the Niobium Bird, including improvements in the signal modeling, hardware upgrades and application of a new nonlinear least squares estimation scheme developed specifically for the Relativity Mission. The improved simulations have achieved 0.12 milliarcsecond errors in the relativistic estimates, providing verification of the science mission's ability to meet its accuracy requirements.

INTRODUCTION

In 1960 L. I. Schiff of the Stanford Physics Department proposed an experiment to test Einstein's General Theory of Relativity using orbiting gyroscopes.[1] He predicted that the spin axis of a gyroscope in a polar orbit would undergo two orthogonal relativistic precessions, known as the geodetic and frame-dragging effects (see Figure 1). The geodetic effect is caused by the warping of space-time by the massive Earth, while the

* Gravity Probe B Relativity Mission, HEPL, Stanford University, Stanford, California 94305-4085.

frame-dragging effect is due to the spinning Earth dragging space-time with it. In a 650 km polar orbit, the magnitude of the geodetic effect is 6.6 arcseconds per year, while the frame-dragging effect is 0.04 arcseconds per year. The Relativity Mission will measure these two precessions with an accuracy of 0.3 milliarcseconds per year. The electrostatically-supported gyroscope must be nearly torque-free to keep the Newtonian precession below this level. Proportional thrusters have been developed to help the satellite achieve nearly drag-free flight and extremely accurate pointing control. The readout system employs a SQUID (Superconducting QUantum Interference Device) magnetometer, an extremely sensitive magnetic field sensor, to determine the gyroscope's spin axis direction.

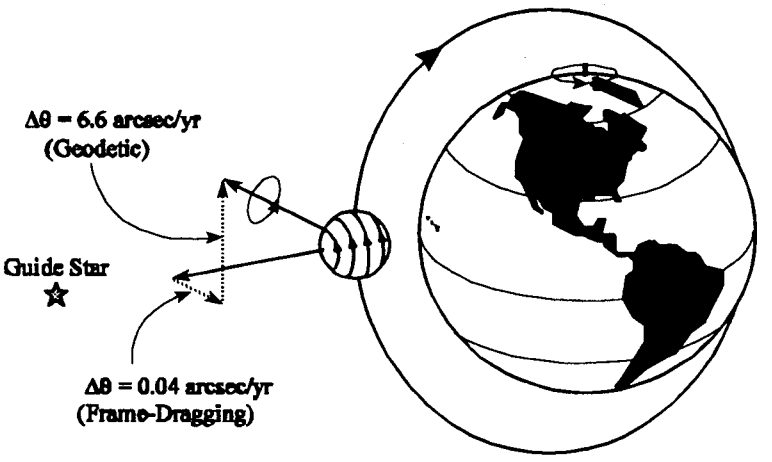

Figure 1 Relativistic Precession Rates of Earth-Orbiting Gyroscope

With the extreme accuracy requirements of the experiment and the myriad of new technologies that must be integrated, it becomes imperative to verify the mission performance as much as possible prior to launch. The Niobium Bird is intended to help provide this verification by integrating computer simulations with prototypical hardware in increasingly realistic hardware-in-the-loop simulations. This report summarizes the latest version of the Niobium Bird, which includes modeling improvements and hardware upgrades. The science mission readout configuration is described first. It is then contrasted with the experimental arrangement found in the Niobium Bird, illustrating the Niobium Bird concept. The truth model computer simulation and the data reduction method are outlined and simulation results are given. The experimental setup is described in detail and results from combined simulation and experiment are given. These results are used to draw conclusions about design considerations for the science mission.

SCIENCE MISSION READOUT

The Relativity Mission experiment consists of three primary systems: 1) telescope, 2) gyroscopes and 3) readout hardware. The telescope provides an inertial reference, from which

the precession of the gyroscopes can be measured, by tracking an inertially fixed guide star. There are four gyroscopes in the mission, each with its own readout hardware. These gyroscopes are quartz spheres coated with niobium, a superconductor at the cryogenic temperatures of the experiment. To achieve the required precision of the experiment, the gyroscopes must be spherical and homogeneous to better than one part in a million. They are electrostatically supported and are spun up by blowing helium gas past the surface. The helium gas is then evacuated to minimize the torque on the gyroscopes. The niobium coating on the gyroscopes gives rise to an effect known as the London moment, which is a magnetic field aligned with the spin axis of a spinning superconductor.

The readout system employs a superconducting pickup loop and a SQUID magnetometer to measure the London moment magnetic field (see Figure 2). The magnetic field generates a current in the superconducting pickup loop. The current is related to the amount of flux passing through the loop, which, in turn, is proportional to the angle that the spin axis makes with the pickup loop (using a small angle approximation). The pickup loop is inductively coupled to the SQUID magnetometer, which operates as a null detector in a feedback loop. This allows the SQUID to track the changing magnetic flux, producing a proportional voltage. This signal passes through an anti-aliasing filter and is then sampled by an A/D converter and sent to the ground, where it is used by the data reduction scheme to infer the direction of the spin axis.

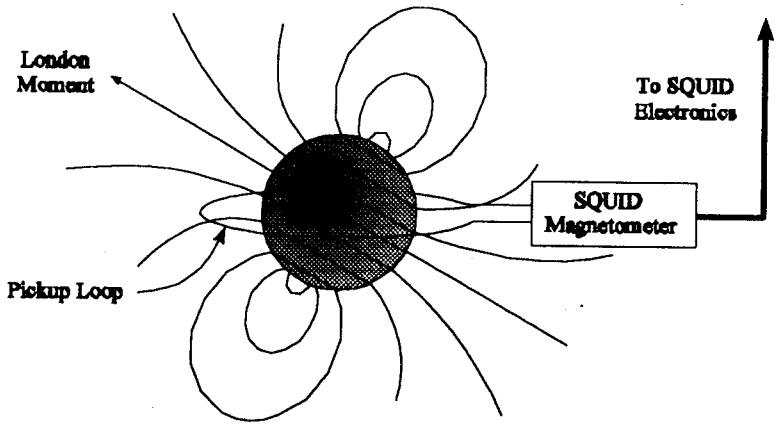

Figure 2 Science Mission Readout System

NIOBIUM BIRD CONCEPT

The purpose of the Niobium Bird project is to provide verification that the Relativity Mission will be able to obtain the desired estimation accuracy for the relativistic drift rates. This is accomplished by simulating the conditions that will be found in the actual science mission. The Niobium Bird differs from the science mission in that the telescope effects and gyroscope signal are numerically simulated, while the prototypical readout hardware and data reduction scheme remain in place. In order to create an actual magnetic flux that can be

measured by the readout hardware, a D/A converter is used to generate a voltage proportional to the simulated gyroscope flux signal. This voltage signal generates a current in a calibration coil, thus creating a magnetic field that emulates the expected gyroscope magnetic signal, as shown in Figure 3 (the gyroscope is still in place, but it is not spinning). This signal is then measured by the prototypical readout hardware, including the pickup loop, SQUID magnetometer and feedback electronics, anti-aliasing filter and A/D converter, after which it can be used by the data reduction scheme to obtain estimates of the relativistic drift rates. It is also important to note that numerical simulations of various portions of the readout hardware are employed in parallel to the experimental verification, increasing the range of investigation and giving extra insight into the underlying processes.

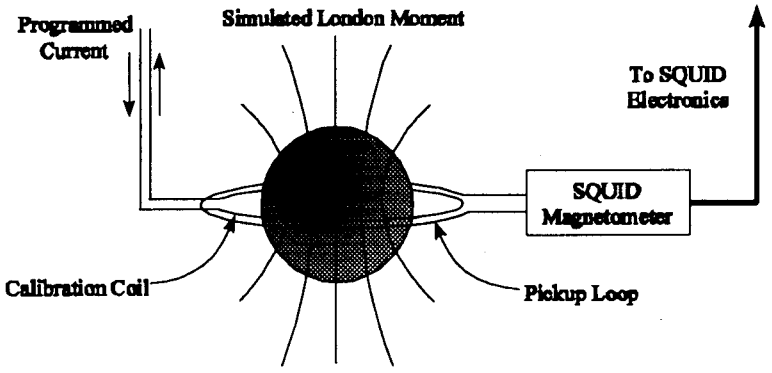

Figure 3 Niobium Bird Readout System

The Niobium Bird concept thus involves the integration of three basic areas: 1) truth model construction 2) experimental verification and 3) data reduction synthesis[3] (see Figure 4). The truth model uses numerical modeling to emulate the gyroscope magnetic flux signal

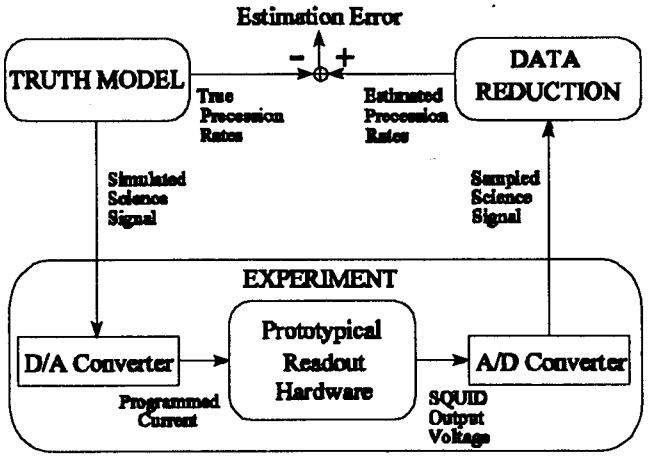

Figure 4 Niobium Bird Conceptual Diagram

that will be produced in the science mission. This simulated data is then converted into a flux signal in the experimental apparatus. The prototypical readout hardware measures the simulated flux and converts it to a voltage signal, which can then be digitized and processed by the data reduction scheme. The resulting estimates are compared to the values used in the truth model to determine the accuracy of the system. The integration of these three facets allows the Niobium Bird to provide an end-to-end verification of the science mission and to serve as a systems engineering tool for establishing an error budget and setting requirements on many aspects of the mission, including gyroscope properties, readout system linearity and telemetry requirements.

TRUTH MODEL CONSTRUCTION

The truth model is a numerical simulation of the magnetic flux signal that occurs at the pickup loop. It also serves as the basis for the measurement model used in constructing the data reduction scheme. The London moment signal can be written as

$$z_f = C_g \delta \tag{1}$$

where the flux z_f is proportional to δ, the angle between the spin axis and the plane of the pickup loop. C_g, the constant of proportionality, is determined by the strength of the London moment and the nature of the pickup loop. Because the satellite is rolled about the reference direction determined by the guide star, the angle between the spin axis and the plane of the pickup loop varies at the roll frequency. This variation makes the two orthogonal relativistic precessions observable. The angle δ can therefore be written as[4]

$$\delta = \left(NS_c + NS_r - \varepsilon_1\right)\cos\left(\omega_r t + \delta\Phi\right) - \left(EW_c + EW_r + \varepsilon_2\right)\sin\left(\omega_r t + \delta\Phi\right) \tag{2}$$

where the orthogonal components of the angle are modulated at the known roll frequency ω_r, which contains an unknown phase shift $\delta\Phi$. The North-South component (the portion of the first term in parentheses) is comprised of an initial misalignment NS_c, the relativistic precession term NS_r, and a time-varying term due to aberration of starlight ε_1. Aberration is a change in the apparent direction of the guide star due to the spacecraft's velocity perpendicular to the line of sight to the guide star. This apparent change in direction is tracked by the telescope, resulting in a motion of the pickup loop relative to the gyroscope. The aberration terms, which contain orbital and annual frequency components, are known quantities, and thus make the scale factor C_g and roll phase $\delta\Phi$ observable. The East-West component of the angle is also comprised of an initial misalignment EW_c, a relativistic precession term EW_r, and a time-varying term due to aberration ε_2. Because the scale factor and roll phase are unknown, the measurement equation is nonlinear in the unknown states. This nonlinear equation forms the basis for the measurement model in the data reduction scheme.

Construction of the truth model also involves modeling potential extraneous flux signals that may be found in the readout system measurements. One such signal arises when magnetic flux from the ambient field is trapped in the gyroscope's niobium coating as it is cooled through its superconducting transition temperature. Despite extensive shielding efforts, there

is always some ambient field which results in this trapped flux. The trapped flux is modeled as point fluxons fixed to the surface of the gyroscope.[5] These fluxons thus generate a signal at the gyroscope spin speed, which is several orders of magnitude greater than the roll rate of the spacecraft. The fluxon magnetic fields have high harmonic content, creating signals at higher harmonics of the spin speed as well.

The position of the fluxons relative to the pickup loop is dependent on the gyroscope's polhoding motion, which is a function of the gyroscope properties. This motion generates a modulation of the spin speed harmonics at harmonics of the polhode frequency, which is very slow due to the homogeneity of the gyroscopes, and a low frequency component that is proportional to the angle between the spin axis and the pickup loop. This low frequency signal thus appears as a variation of the London moment scale factor at harmonics of the polhode frequency. It can be added to the London moment signal given in Eq. (1) as follows

$$z_t = \left(C_g + C_{tf}\right)\delta \tag{3}$$

where C_{tf} is a time-varying scale factor composed of polhode harmonics, which, as an unmodeled signal, can create estimation errors due to partial masking of the London moment. Figure 5 shows a typical trapped flux scale factor variation for 50 trapped fluxons with a five-turn pickup loop and 130 Hz gyroscope spin rate. The scale factor variation is periodic at the polhode period, which is approximately 30.8 minutes for this case. The London moment scale factor, in terms of flux in the loop, is approximately 0.11 Φ_0/arcsec (1 Φ_0, or flux quantum, is equal to 2.07×10^{-7} Gauss•cm^2). Thus, the scale factor variation for this particular fluxon distribution is on the order of 0.1% of the London moment scale factor.

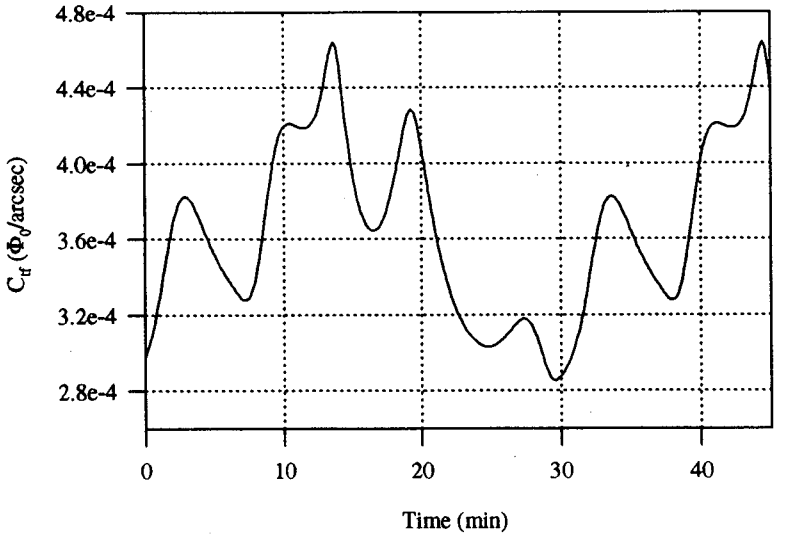

Figure 5 Typical Trapped Flux Scale Factor Variation

In addition to this low frequency signal, the truth model also simulates the high frequency components of the trapped flux signal. The purpose of the anti-aliasing filter in the

science mission is to remove these high frequency signals from the data so that only the desired low frequency signal remains. Nonlinearities in the readout hardware, however, can cause intermingling of these high frequencies to produce low frequency signals, which can again interfere with the London moment signal. The effects of both high and low frequency components of the trapped flux signal will be addressed in the following sections. Other extraneous flux signals, such as suspension system coupling and external field leakage, have been or will be included in the truth model construction of the Niobium Bird, but are not addressed in this paper.

DATA REDUCTION SYNTHESIS

The data reduction scheme used in the Niobium Bird is a new nonlinear least squares estimator developed specifically for the Stanford Relativity Mission.[6] The reason for developing the new method was that most available nonlinear least squares estimation algorithms require a choice between an optimal solution, usually involving batch fit methods,[7] and a recursive scheme, as in the case of the extended Kalman filter and the iterated extended Kalman filter.[8] In contrast, the new estimator developed for the Relativity Mission obtains the optimal estimate with a recursive algorithm. The problem of minimizing the quadratic (least squares) cost function is divided into two steps by defining intermediate, or first step, states that are nonlinear combinations of the desired, or second step, states. This is done in such a way that the first step becomes a linear problem and estimates of the first step states can be found using a linear Kalman filter. The second step states are then found by performing a nonlinear least squares fit to the first step estimates.

To create the measurement model on which the data reduction scheme is based, we assume that the readout system makes a linear measurement of the London moment flux signal (extraneous signals such as the trapped flux are left unmodeled). The measurement can be written as

$$z = C_s z_f + b + v \tag{4}$$

where C_s is the scale factor associated with the readout system, b is the readout bias, and v is measurement noise, which is assumed to be a zero-mean, white gaussian process. Substituting Eqs. (1) and (2) into Eq. (4) and writing the relativistic terms as constant drift rates, the measurement equation becomes

$$z = C_s C_g \left[\left(NS_c + A_g t - \varepsilon_1 \right) \cos\left(\omega_r t + \delta\Phi\right) - \left(EW_c + A_f t + \varepsilon_2 \right) \sin\left(\omega_r t + \delta\Phi\right) \right] + b + v \tag{5}$$

where A_g and A_f are the geodetic and frame-dragging drift rates, respectively. One complicating factor in this measurement equation involves the occultation of the guide star by the Earth during approximately half of the satellite's orbit. Because the telescope cannot track the guide star during occultation, it has no information about the relativistic drift rates and hence this period is ignored by the data reduction scheme.

From the measurement equation, we can define the desired unknowns, or second step states, as

$$\mathbf{x} = \begin{bmatrix} C \\ NS_c \\ EW_c \\ A_g \\ A_f \\ \delta\Phi \\ b \end{bmatrix} \tag{6}$$

where the readout and London moment scale factors have been combined into one scale factor C. All of the unknown states are modeled as constants in the filter. Drifting in the scale factor and roll phase parameters can occur in the experiment. The ability to track these drifts using a random walk process noise model has been added to the data reduction algorithm.[6] The work presented in this paper, however, treats these drifts as unmodeled errors.

The next step is to rewrite the measurement equation in the form required by the two-step estimation algorithm described in Ref. 6. Using trigonometric identities to substitute for the sine and cosine terms, Eq. (5) can be rearranged to create a linear problem as follows

$$z = H(t)\mathbf{y} \tag{7}$$

where

$$H^T = \begin{bmatrix} \cos(\omega_r t) \\ \sin(\omega_r t) \\ t\cos(\omega_r t) \\ t\sin(\omega_r t) \\ \varepsilon_1 \cos(\omega_r t) + \varepsilon_2 \sin(\omega_r t) \\ \varepsilon_1 \sin(\omega_r t) - \varepsilon_2 \cos(\omega_r t) \\ 1 \end{bmatrix}. \tag{8}$$

and

$$\mathbf{y} = \mathbf{f}(\mathbf{x}) = \begin{bmatrix} C\left(NS_c \cos(\delta\Phi) - EW_c \sin(\delta\Phi)\right) \\ -C\left(NS_c \sin(\delta\Phi) + EW_c \cos(\delta\Phi)\right) \\ C\left(A_g \cos(\delta\Phi) - A_f \sin(\delta\Phi)\right) \\ -C\left(A_g \sin(\delta\Phi) + A_f \cos(\delta\Phi)\right) \\ -C\cos(\delta\Phi) \\ C\sin(\delta\Phi) \\ b \end{bmatrix} \tag{9}$$

where the first step states $\mathbf{y}$ are nonlinear functions of the unknown second step states $\mathbf{x}$, while the measurement matrix $H(t)$ contains only known quantities. Since the first step states enter the measurement equation linearly, a linear Kalman filter will yield optimal estimates of these

parameters.[9] The second step states are then optimally obtained from the estimates of the first step states using an iterative Gauss-Newton batch fit.[7] The static two-step algorithm can be summarized as follows:

First Step Estimation (Static Kalman Filter)

$$\hat{\mathbf{y}}_k = \hat{\mathbf{y}}_{k-1} + P_{y_k} H_k{}^T R_k{}^{-1}(z_k - H_k \hat{\mathbf{y}}_{k-1}) \qquad k = 1 \ldots N$$

$$P_{y_k} = (P_{y_{k-1}}{}^{-1} + H_k{}^T R_k{}^{-1} H_k)^{-1}$$

Second Step Estimation (Gauss - Newton Batch Fit)

$$\hat{\mathbf{x}}_{k,i+1} = \hat{\mathbf{x}}_{k,i} - \mathrm{H}_{G_{k,i}}{}^{-1} q_{k,i}{}^T$$

$$\mathrm{H}_{G_{k,i}} = \left.\frac{\partial \mathbf{f}}{\partial \mathbf{x}}\right|^T_{\mathbf{x}=\hat{\mathbf{x}}_{k,i}} P_{y_k}{}^{-1} \left.\frac{\partial \mathbf{f}}{\partial \mathbf{x}}\right|_{\mathbf{x}=\hat{\mathbf{x}}_{k,i}} \qquad k = 1 \ldots N$$

$$q_{k,i} = -(\hat{\mathbf{y}}_k - \mathbf{f}(\hat{\mathbf{x}}_{k,i}))^T P_{y_k}{}^{-1} \left.\frac{\partial \mathbf{f}}{\partial \mathbf{x}}\right|_{\mathbf{x}=\hat{\mathbf{x}}_{k,i}}$$

$$P_{x_{k,i}} \approx \mathrm{H}_{G_{k,i}}{}^{-1}$$

where k represents the measurement number, i represents the iteration number and there are N total measurements. R is the covariance of the measurement noise, while P_y and P_x represent the covariance matrices associated with the first and second step states, respectively; q and H_G are, respectively, the Jacobian (or gradient) and Hessian (or curvature) matrices associated with the vector of functions $\mathbf{f}$. The first step is decoupled from the second step, which means the second step can be performed off-line. For the case of time-varying unknowns, the two steps become coupled and the method no longer guarantees the optimal solution.[6]

The advantage of using the two-step method is that, for the case of constant unknown states, no linearization is necessary in finding the first step states, while the second step states can be found optimally off-line at any time. In contrast, the extended Kalman filter and iterated extended Kalman filter require linearization about the previous iteration's estimate at each step, resulting in suboptimal estimates.[6]

SIMULATION RESULTS

A baseline from which to judge the hardware performance and the importance of unmodeled effects (such as trapped flux) can be established by generating simulated measurements using the measurement model of Eq. (5), including simulated SQUID noise at the levels measured in the lab. These simulated measurements are fed directly into the data reduction scheme, yielding the best possible estimate given this measurement model. Figure 6 shows how the filter estimate converges over time for a single Monte Carlo run of this type. For a one year simulation, we have obtained 0.12 milliarcsecond errors in the relativitistic drift rate estimates using this method (for a 130 Hz gyroscope spin rate).

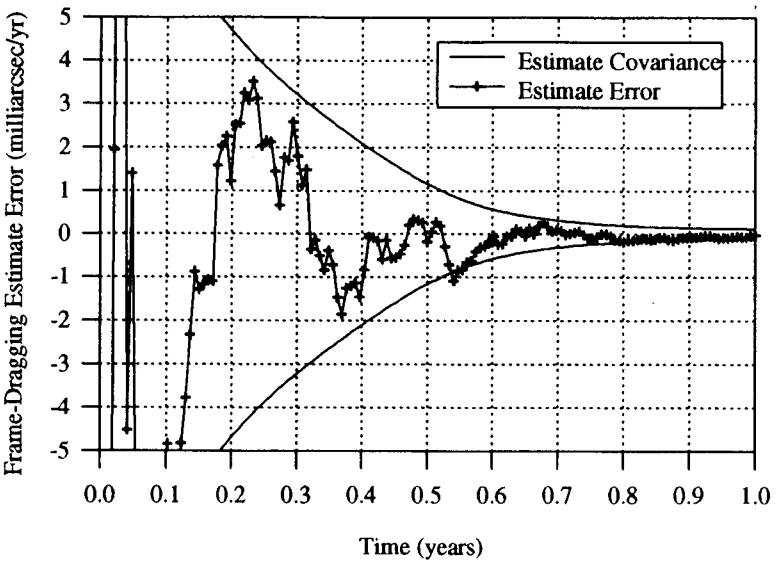

Figure 6 Estimation Error for Typical Monte Carlo Run

The next step is to investigate the effects of extraneous signals in the truth model (and, eventually, the readout hardware) that are not modeled in the filter. One such effect is the trapped flux described above. The low frequency signal added by the trapped flux can lead to signals that look like the London moment signal and thus add to the estimation error. As stated before, the trapped flux appears as a low frequency variation of the London moment scale factor at harmonics of the gyroscope polhode frequency. We have found that this can create errors in the relativistic estimates when a polhode harmonic approaches one of the harmonics of the orbital frequency. These errors are caused by terms created when the trapped flux scale factor C_{tf} multiplies the term containing the orbital aberration ε_1. The mixing of these two frequencies creates new terms at the sum and difference of the polhode harmonics and the orbital frequency. This signal is further complicated by the fact that only half the orbit is used in the data reduction scheme, which introduces orbital harmonics into the measurement equation. The result is the creation of signals that have the same time signature as the orbital aberration itself, affecting the scale factor estimate and leading to errors in the drift rate estimates.

Figures 7 and 8 show how the final errors in the relativistic drift rate (in this case, the frame-dragging drift, although the geodetic estimates exhibit similar results) vary with the polhode frequency of the gyroscope. Figure 8 provides greater resolution of a portion of the horizontal axis from Figure 7. When the ratio of the orbit period to the polhode period is an integer or a simple fraction (e.g., 7/3), large errors occur. This is an indication of mixing of a polhode harmonic with an orbit harmonic to give a signal that looks like the orbital aberration. The width of these peaks, an indication of how close the polhode harmonic must be to the orbital harmonic, decreases as the length of the experiment increases. Figure 8 illustrates that these error peaks are very narrow and occur both at integer values and at simple

fractions. After one year, the probability of getting a polhode period that lands on one of the peaks is a fraction of a percent. In between the peaks, the error from this signal is much smaller than that due to SQUID noise and can be left unmodeled. In the unlikely event that the gyroscope polhode period should happen to land on one of the peaks, there are several possible ways to fix the problem, including changing the gyroscope spin speed (which is directly proportional to the polhode frequency), changing the orbital frequency, or including the trapped flux polhode harmonics in the filter model.

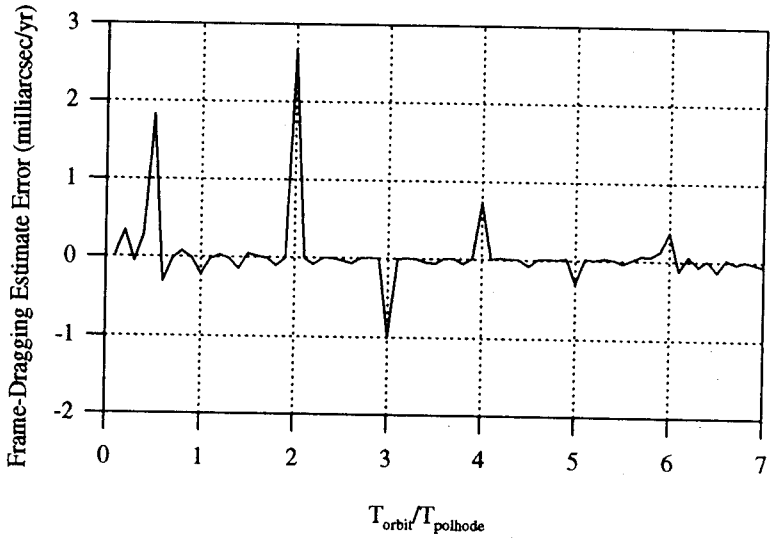

Figure 7 Estimation Errors Due to Low Frequency Trapped Flux Signal

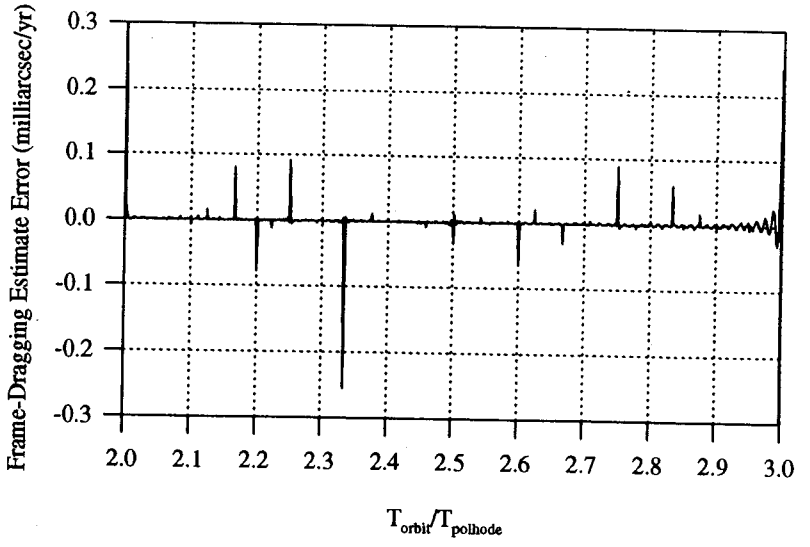

Figure 8 Close-Up of Estimation Errors Due to Trapped Flux Signal

Two major concerns have been addressed in this paper. The first is the trapped flux, which generates an extraneous flux signal. The second is the nonlinearity of the readout system, which can also create unmodeled signals in the measurements. These two error sources have been analyzed in both simulation and experiment. We have shown that the resulting errors depend primarily on the polhode frequency of the gyroscope. These errors can be ignored for most polhode frequencies, and the polhode frequency can be changed or modeled in the filter if an undesirable frequency occurs. Thus the error due to SQUID measurement noise, 0.12 milliarcseconds per year, remains the dominant error.

With its integrated environment, the Niobium Bird will continue to provide excellent opportunities to verify the performance of the Relativity Mission. Future work will include improvements of the truth model, including more sophisticated trapped flux modeling as well as modeling of other potential flux sources. The experiment will be continually upgraded to include the most prototypical hardware available. In addition, other portions of the science mission equipment, such as the on-board processing and telemetry hardware, can be included. The data reduction method is also being improved to include modeling of extraneous signals and to allow for state dynamics. The hardware-in-the-loop concept of the Niobium Bird will allow it to continue to provide verification that these various facets of the science mission can be integrated to achieve the required accuracy for the relativity parameters.

ACKNOWLEDGEMENT

This work was prepared under NASA contract NAS8-39225.

REFERENCES

1. L. I. Schiff, "Possible New Experimental Test of General Relativity," *Physical Review Letters*, Vol. 4, 1960, pp. 215-217.
2. C. W. F. Everitt, "The Stanford Relativity Gyroscope Experiment (A): History and Overview," in *Near Zero: New Frontiers of Physics*, J. D. Fairbank, J. B. S. Deaver, C. W. F. Everitt and P. F. Michelson, Eds., W. H. Freeman and Company, New York, 1988, pp. 587-639.
3. H. Uematsu, *The Gravity Probe B Niobium Bird Experiment: Experimental Verification of a Data Reduction Scheme With a Prototypical DC SQUID Readout System*, Ph.D. Dissertation, Stanford University, Stanford, CA, 1993, SUDAAR 639.
4. N. J. Kasdin, *Precision Pointing Control of the Spinning Gravity Probe B Spacecraft*, Ph.D. Dissertation, Stanford University, Stanford, CA, 1991, SUDAAR 606.
5. L. L. Wai, "The Effect of Trapped Magnetic Flux Quanta on the London Readout in GP-B," B.S. Honors Thesis, Stanford University, Stanford, CA, 1989.
6. G. T. Haupt, N. J. Kasdin, G. M. Keiser and B. W. Parkinson, "An Optimal Recursive Iterative Algorithm for Discrete Nonlinear Least Squares Estimation," submitted to *AIAA Journal of Guidance, Control, and Dynamics*, Nov. 1994.
7. Y. Bard, *Nonlinear Parameter Estimation*, Academic Press, New York, 1974.
8. A. Gelb, *Applied Optimal Estimation*, M.I.T. Press, Cambridge, MA, 1974.
9. A. E. Bryson and Y. C. Ho, *Applied Optimal Control*, Hemisphere, New York, 1975.